

Simulation of Electric Propulsion Thrusters

Iain D. Boyd*

Department of Aerospace Engineering
University of Michigan
Ann Arbor, Michigan, USA

iainboyd@umich.edu

ABSTRACT

Electric propulsion thrusters are replacing small chemical thrusters used for spacecraft control and orbital maneuvers. These thrusters use a variety of mechanisms to convert electrical power into thrust and in general provide superior specific impulse in comparison to chemical systems. Electric propulsion has been under development for the last fifty years, and almost all thrusters are designed based largely on experience and experimentation. The present article considers the progress made in numerical simulation of electric propulsion thrusters. Due to the wide range of such devices, attention is restricted to electric propulsion thruster types that are presently in use by orbiting spacecraft. The physical regimes created in these thrusters indicate that a variety of numerical methods are required for accurate numerical simulation ranging from continuum formulations to kinetic approaches. Successes of numerical simulation models are demonstrated through specific examples. It is concluded that numerical simulations can be expected to play a more prominent role in the design and evolution of future electric propulsion thrusters.

1.0 INTRODUCTION

Electric propulsion technology generates thrust primarily from electrical energy through a number of different mechanisms. In general, electric thrusters provide superior performance for spacecraft propulsion in comparison to chemical thrusters due to their significantly higher specific impulses. The advantage of high specific impulse propulsion can be understood from the rocket equation:

$$\frac{M_f}{M_i} = \exp\left(-\frac{\Delta V}{gI_{sp}}\right) \quad (1.1)$$

where M_i and M_f are the initial and final spacecraft masses, respectively, ΔV is the required change in spacecraft velocity for the mission, g is the gravitational acceleration (at the Earth's surface), and I_{sp} is the specific impulse. Equation (1.1) indicates that to maximize useful payload, we want to maximize the specific impulse. While propulsion systems based on chemical propellants are limited to I_{sp} in the range of 200-400 sec, electric propulsion systems generate I_{sp} in the range of several hundred to several thousand seconds. Table 1 lists typical values of specific impulse and thrust associated with several types of electric propulsion systems. In addition to superior propellant mass efficiency, electric propulsion is ideal for providing very low impulse bits required by high-resolution observing missions and by spacecraft constellations. There are two categories of activities involving numerical modelling of electric thrusters. The first concerns modelling of

* Approved for public release; distribution unlimited

the thruster device and its acceleration processes. The primary goal of these activities is to aid in the fundamental understanding of the physical mechanisms of the thruster with the objective of improving its performance in terms of propulsion efficiency and operational lifetime. The second area of modelling activity concerns the plumes produced by electric thrusters. Detailed information on the plumes is required for safe integration of the thruster onto a spacecraft. Modelling plays an important role here because it is problematic and expensive to reproduce the in-orbit space environment using ground-based laboratory facilities. Device modelling also plays an important role in plume simulations by providing accurate boundary conditions at the thruster exit. The present article is focused on the numerical simulation of the flows in electric propulsion thrusters.

While there is ample motivation for the use of numerical modelling in electric propulsion, much of the thruster design and spacecraft integration work continues to be experimental and empirical. This is largely due to the technical challenges of creating physically accurate models of these complex systems. In this article, the current state of the art for numerical modelling of the device flows of a variety of electric thrusters is reviewed. Due to space limitations, the focus is restricted to thruster types that are presently operating in space. Thus, the thrusters considered are resisto-jets, arc-jets, gridded electro-static ion thrusters, and Hall effect thrusters. Several other thruster types are therefore omitted including magnetoplasmadynamic (MPD) thrusters, pulsed plasma thrusters, thrusters based on electro-magnetic wave sources, field emission electric propulsion (FEEP), colloid thrusters, and laser-based thrusters. The fundamental physical characteristics of the thrusters considered are discussed to illustrate the types of numerical approaches required to accurately model the most important phenomena. It will become clear that some thrusters can be modelled using a continuum formulation while others require a kinetic approach. Wherever appropriate, the strengths and weaknesses of the existing models for these thrusters are discussed.

Finally, the future prospects for improvement in numerical modelling of electric thrusters are considered. As with many technological areas, the potential for numerical modelling in the design, optimization, and integration of electric thrusters is significant. However, the physical complexity of many of these thrusters makes the goal of developing accurate numerical models one that still requires much fundamental research. Specific areas where advances are required in the modelling are discussed.

2.0 NUMERICAL METHODS

The focus of this article is on numerical methods used to model the flow of gas and plasma through electric propulsion devices. Discussion of the numerical analysis of other aspects of thruster design, such as thermal and structural processes, is omitted here. There are two fundamental types of numerical approaches for modelling these gas and plasma flows: (1) continuum or fluid methods, and (2) kinetic methods. The choice of method for modelling a specific thruster should be dictated by the physical characteristics of the flow in the device, and by the level of accuracy required from the simulation. As we shall see, there is a wide range of conditions in different types of thrusters. In general this means that different methods and computer codes must be developed for each of the different thrusters. Before considering models for the various thrusters, let us first review the most important numerical methods that are employed.

2.1 Continuum/Fluid Methods

The gas or plasma may be considered as a continuum or fluid when length scales associated with the most important physical phenomena (spatial gradients of flow properties, distance between collisions, charge

separation distance) are small in comparison to the size of the thruster. In general, these conditions are encountered in the relatively high density devices such as resisto-jets and arcjets. Continuum methods are usually based on a set of partial differential equations describing conservation of mass (or charge), momentum, and energy. For example, the viscous flow encountered in a resisto-jet may be modelled using the following equation set (often referred to as the Navier-Stokes equations):

$$\text{Continuity: } \frac{\partial \rho}{\partial t} + \frac{\partial \rho u_j}{\partial x_j} = S_C \quad (2.1)$$

$$\text{Momentum: } \frac{\partial \rho u_i}{\partial t} + \frac{\partial \rho u_i u_j}{\partial x_j} = -\frac{\partial p}{\partial x_i} + \frac{\partial \tau_{ik}}{\partial x_k} + \rho F_i + S_{M_i} \quad (2.2)$$

$$\text{Energy: } \frac{\partial \rho e}{\partial t} + \frac{\partial \rho u_j e}{\partial x_j} = \frac{\partial p}{\partial t} + \frac{\partial}{\partial x_k} [u_j \tau_{jk} - q_k] + \rho F_i u_i + S_E \quad (2.3)$$

where ρ is the mass density, u_i is a velocity component, p is the pressure, e is the total specific internal energy, τ_{ik} and τ_{jk} are shear stress tensors, q_k is the heat flux vector, F_i is an external body force, and S_C , S_{M_i} , and S_E are source terms caused by chemical reactions in the mass, momentum, and energy equations, respectively. First-order models for the shear stress and heat flux vector use temperature-dependent transport coefficients (viscosity and thermal conductivity). For plasma flows, additional equations supplement the above set. These additional equations are highly specific to the particular thruster type. In general, it is necessary to include an additional set of conservation equations for the electrons and to add terms to the heavy particle momentum equation to account for the electro-magnetic fields and friction with the electrons. Equation sets of this type can be solved using a wide variety of numerical approaches. In *finite difference* formulations, each partial derivative is evaluated to some order using Taylor expansions. In *finite volume* formulations, the integral forms of the conservation equations are solved. The issues regarding these formulations are discussed in a variety of texts, e.g. Tannehill, Anderson & Pletcher [1], Fletcher [2].

2.2 Kinetic Methods

The flows in many electric propulsion systems fall into the rarefied regime in which collision and plasma length scales are similar to or even larger than the size of the thruster. In such cases, the flow is not well represented by a continuum formulation, and instead, a molecular, kinetic approach must be undertaken. Let us discuss separately the numerical simulation of rarefied gas-dynamic and plasma-dynamic effects.

2.2.1 Gas Dynamics

The Knudsen number is defined as the ratio of the mean free path (the average distance travelled by each molecule between successive collisions) and the characteristic length of the flow (e.g. the diameter of a thruster). In general, the rarefied flow regime is defined to exist for Knudsen numbers above 0.01. The continuum approach fails under rarefied conditions because there is an insufficient rate of collisions to maintain the velocity distribution functions anywhere near to the small departures from the Maxwellian equilibrium form implicitly assumed in continuum formulations. While, in principle, the Boltzmann equation of dilute gas dynamics should be solved under high Knudsen number conditions, this turns out to be a formidable mathematical and computational task. The direct simulation Monte Carlo method (DSMC) of Bird

[3] is a well-developed, highly successful numerical technique for simulating rarefied gas flows. In this technique, no attempt is made to solve any specific governing equation. Instead, a direct simulation of the molecular-level gas dynamics is performed. In the DSMC technique, a large number of model particles is simulated. Each model particle represents a much larger number of real atoms or molecules. The model particles possess unique velocity components. A key aspect of the DSMC technique is that particle motion is decoupled from particle collisions. This is only reasonable if the time step employed in the simulation is significantly smaller than the mean time between collisions. Thus, during each iteration of the DSMC algorithm, all the particles are first moved according to the product of the time step and their individual velocity vectors. Any interactions between the particles and boundaries are then processed. The particles are next collected into cells for computation of collisions. Within each cell, the positions of the particles are ignored. Instead, the particles are paired up at random and collision probabilities are computed for each pair to determine whether a collision occurs. This statistical approach is only accurate when the size of the computational cell is of the order of a mean free path. The collision probability is proportional to the product of the collision cross section and the relative velocity of the colliding particles. Many different types of collision phenomena can be simulated using the DSMC technique including momentum exchange, charge exchange, internal energy exchange, and chemical reactions. Average flow properties such as density, velocity, and pressure are obtained by time-averaging of the particle properties. Unsteady flows may be simulated by averaging over small periods of time, or by ensemble averaging. A related method, the Monte Carlo Collision (MCC) technique [4], is also often used in electric propulsion simulations. This approach is useful in hybrid particle-fluid simulations to determine the effects of collisions of electrons (modelled as a fluid) on the heavy species that are represented as particles.

2.2.2 Plasma Dynamics

Similar to gas flow, a plasma cannot be described accurately by a continuum formulation under high Knudsen number conditions. However, continuum models can still yield useful solutions in cases where the underlying collision effects are dominated by the plasmadynamics. For electric propulsion devices, the most important behaviour to simulate is the plasmadynamic effects on the momentum of the heavy ions since these are the main source of thrust. The Particle In Cell (PIC) method, see Birdsall and Langdon [5], is a particle technique for simulating plasmas. In most electric propulsion systems, ions are treated as particles using PIC and the electrons are treated using a continuum, fluid approach. This approach is usually justified as the time scales associated with the much lighter electrons are orders of magnitude smaller than those for the heavy ions. In addition, even if the velocity distribution function of the electrons is not Maxwellian, it is usually compact allowing meaningful interpretation of continuum quantities such as temperature and pressure. Plasma physics has been described as the art of approximation, and this is an important aspect of applying the PIC method to electric propulsion flows. The underlying philosophy should always be to take the simplest approach that provides adequate results. Wherever possible, the assumption of charge quasi-neutrality is employed. This approach allows the spatial distribution of the ions to give the spatial distribution of the electrons. This is a good assumption provided the Debye length, the distance over which electrons and ions are shielded from one another, is much smaller than the length scale of the thruster. For a typical thruster electron temperature of several electron-volts, the assumption of quasi-neutrality is good down to plasma densities of about 10^{14} m^{-3} that is much lower than values encountered in most electric propulsion thrusters (see values listed in Table 1) except for the inter-grid regions of ion thrusters. A variety of approximations of the electron momentum and energy equations are invoked for different types of electric propulsion thrusters. These will be discussed for each thruster type. The electric field is usually obtained from spatial differentiation of the plasma potential that in turn is derived from the electron momentum equation. This field is used to change the velocity vector of each ion particle in the PIC simulation according to Newton's 2nd Law:

$$m_i \frac{d\bar{v}}{dt} = q_i \bar{E} \quad (2.4)$$

where m_i is the ion mass, \bar{v} is the ion velocity vector, q_i is the ion charge, and \bar{E} is the electric field. The steps in the PIC algorithm are to obtain the plasma density from the spatial distribution of the ions, calculate the electric field, accelerate the ions, and finally move the ions. Note that the DSMC calculation of ion collisions is very easily introduced into the PIC algorithm after the movement step.

3.0 THRUSTER MODELS

In the following sections, a summary is provided of the past history and current status of numerical modelling of four different types of electric propulsion thrusters presently operating in space.

3.1 Resistive-Jets

A resistive-jet is classified as an electrothermal device. It operates by flowing gaseous propellant over an electrical element that raises the gas temperature. The heated gas is accelerated gas dynamically through a converging-diverging nozzle to produce thrust. As of May 2010, there were more than 100 operational spacecraft using hydrazine resistive-jets in space. Resistive-jets typically have good efficiencies of 70-80%. The key performance loss mechanisms concern the development of relatively large viscous boundary layers along the nozzle wall (caused by the relatively low gas density), and frozen flow losses caused by the freezing of energy into internal modes such as rotation and vibration.

The physical characteristics of a typical resistive-jet involve a number density at the nozzle exit of 10^{21} m^{-3} , a velocity of 1-5 km/s, and an exit diameter of a few centimetres. These values give a Knudsen number at the nozzle exit of about 0.1 that indicates the gas flow involves transition from continuum flow at the nozzle throat, to rarefied flow at the nozzle exit. Numerical simulations of resistive-jets have employed both continuum and kinetic methods. For example, Kim [6] solved the Navier-Stokes equations using a steady, finite-volume formulation. Full DSMC computations of the nozzle flows of cold and hot resistive-jet flows were performed by Boyd et al. [7,8]. Figure 1 shows Mach number contours computed using DSMC in the diverging nozzle of a cold-flow hydrogen resistive-jet [8]. Such computations typically are begun at the nozzle throat assuming sonic conditions. The contours clearly illustrate the thick, viscous boundary layer formed along the nozzle wall. Figure 2 provides a comparison between experimental measurements (obtained using Coherent Anti Raman Scattering, CARS) and DSMC simulation for the velocity along the axis of the hydrogen resistive-jet [8]. Simulations and experimental measurements are again compared in Fig. 3 for specific impulse. The simulations agree within 5% of the measured data. A comparison between data obtained with the Navier-Stokes equations, with the DSMC method, and with experimental measurements of pitot pressure was conducted by Boyd et al. [7]. It was found that the DSMC computations offered superior agreement with the measurements to those obtained with the CFD analysis.

As demonstrated by the results shown in Figs. 2, 3, the accuracy of numerical simulations for resistive-jet flows is high due to the relative simplicity of the physical phenomena that occur in this device. Thus, computational analysis can be used with confidence to aid in the design of new resistive-jets. This is the approach taken for the Free-Molecule Microresistivejet developed for low thrust levels that has been designed extensively by Ketsdever et al. [9] using the DSMC technique. Computed values for performance parameters were found to agree with experimental measurements to within 2-4% for different propellants.

Although many resisto-jets are presently operating in space, interest in further development of this thruster type has declined since significantly superior performance are offered by the other forms of electric propulsion thrusters. Specialized resisto-jet systems have been developed and tested in recent years that use water, xenon, and ammonia as propellants for small spacecraft [10,11,12].

3.2 Arcjets

An arcjet thruster is also an electrothermal device. It operates by flowing gas through an electrical arc formed between a cathode placed near the throat of a nozzle, and the nozzle itself that acts as the anode. The arc transfers energy to the gas through the Ohmic (Joule) heating mechanism, and the hot gas is subsequently accelerated through a diverging nozzle. As of May 2010, there were more than 40 operational spacecraft using hydrazine arcjets in space. The efficiency of an arcjet is only about 30% and is significantly lower than for a resisto-jet due to more significant frozen flow losses. These losses result from a variety of nonequilibrium collisional phenomena that occur in arcjet nozzle flows including rotational and vibrational energy relaxation, dissociation of molecules, and ionization of atoms. As illustrated in Table 1, however, arcjets do offer significantly higher specific impulse than resisto-jets.

Arcjets developed for space propulsion typically operate at power levels of 1 to 10 kW using hydrazine propellant, and have physical characteristics that are similar in density to resisto-jets, although the velocity is usually higher, resulting in the higher specific impulses. Most arcjet device models are based on a continuum approach in which the continuum conservation equations are solved together with appropriate transport coefficients. Butler and King [13] developed a two-fluid model of a 10 kW hydrogen arcjet that used separate continuity, momentum, and energy equations for the heavy particles and the electrons. The fluid equations were augmented with basic plasma relations such as Faraday's law, Maxwell's equation for the magnetic field, and Ohm's Law for Joule heating. In a similar approach, Miller and Martinez-Sanchez [14] solved a continuity equation for each species, momentum equations for the axial, radial, and azimuthal coordinates, and energy equations for the electrons and the heavy particles that included Ohmic heating, and losses due to electron collisions and radiation. In addition, dissociation and ionization reactions for the hydrogen propellant were included. These models typically offer agreement within 10% of measured performance data. A similar arcjet model was presented by Megli et al. [15] for hydrazine propellant by implementing a finite rate, nonequilibrium, chemical kinetics mechanism for the N_2-H_2 system. Models developed for high power arcjets (100 kW) by Auweter-Kurtz et al. [16] add magnetic effects to the momentum and energy equations, and a separate energy equation for the vibrational energy of molecules. One example of a particle-based kinetic description of arcjets was developed by Boyd [17,18] in which the usual DSMC technique for a multi-species, reacting gas, is augmented by a kinetic model for Ohmic heating. Continuum and DSMC methods were applied to investigate the effects of nozzle geometry on arcjet design by Hatta and Aso [19].

The accuracy of numerical simulations for arcjet flows is much less than that for resisto-jets due to the significantly wider range of physical processes that are involved. The reduction in accuracy stems mainly from a lack of information on some of these physical processes such as molecular transport coefficients in a nonequilibrium plasma. Figure 4 (taken from Boyd [18]) shows the decoupled flow domain in which a continuum approach is employed up to the nozzle throat that is used as a start line for the DSMC analysis. The nozzle wall temperatures are also taken from the continuum model. Figures 5 and 6 show comparisons of axial and radial velocity profiles in a 1.4 kW hydrogen arcjet. The measured data were obtained using Laser Induced Fluorescence. The agreement between the predicted and measured data is quite good. Comparison between the DSMC simulation (with and without Ohmic heating Ω) and measurement of specific impulse is shown in Fig. 7 where the agreement between the datasets is within 10%.

Similar to resisto-jets, although many arcjets are presently operating in space on communications satellites, interest in further development of this thruster type has declined since significantly better performance is offered by ion and Hall thrusters. Notable exceptions include development of arcjets for lunar and planetary exploration [20, 21]. In addition, similar to other EP devices, arcjet designs have been scaled down for small satellite applications [22].

3.3 Ion Thrusters

A gridded ion thruster is an electrostatic device that operates by flowing gas propellant (usually xenon or krypton) into a *discharge chamber* where a *hollow cathode* provides electrons that ionize the gas. The resulting plasma then drifts towards a set of grids (usually two: a *screen grid* and an *acceleration grid*) across which a large potential difference is applied in order to accelerate the ions to very high velocity. The ions flow through the grids via a large number of small apertures, each of which focuses the ions, and is therefore called the *ion optics*. A schematic diagram of an ion thruster is provided in Fig. 8 that shows the main components. In the following, the status of modelling is reviewed of the major ion thruster components, namely the *discharge chamber*, the *hollow cathode*, and the *ion optics*. As of May 2010, there were more than 30 operational spacecraft using xenon gridded ion thrusters in space. Notable applications of ion thrusters include Deep Space-1 (NASA), Dawn (NASA), Hayabusa (JAXA) and the XIPS system used on Boeing communications satellites. The efficiency of an ion thruster is typically about 70%. The primary loss mechanisms are the propellant ionization and beam divergence. Another key issue in the use of this type of electric propulsion system is thruster lifetime. Some of the ions accelerating through the grids can impinge on the grids at energies that are sufficiently large to cause sputtering of the grid material. After several thousand hours of operation, the grids can become completely eroded away, leading to failure of the thruster.

3.3.1 Discharge Chamber

A key step in ion thruster design involves achieving uniform plasma conditions in the discharge chamber, and this is largely controlled by employing a magnetic field topology that constrains the electron trajectories so as to enhance ionization. A complete model of the discharge chamber of an ion thruster was first developed by Arakawa and Ishihara [23] using a combination of a finite element fluid approach and a Monte Carlo method for the primary electrons that originate from the cathode. Ions were treated as a fluid, electro-static fields were ignored, and secondary electrons (those created in the ionization process) were omitted. In a more advanced approach, Jugroot and Harvey [24] applied a combination of the DSMC and fluid plasma methods to analyze the discharge chamber of the UK-T5 ion thruster.

Wirz and Katz [25] describe the development of a comprehensive axially symmetric discharge chamber model that treats the primary electrons as particles using PIC, while the ions and secondary electrons are described using a fluid description. The neutral gas is modelled using sources and sinks based on expressions from kinetic theory. An even more comprehensive modelling approach is described by Mahalingam and Menart [26] in which ions, primary electrons, and secondary electrons are all treated as particles using PIC while a uniform neutral gas distribution is assumed. Stueber [27] describes the development of a three-dimensional, particle-based simulation technique for mapping the neutral atom distribution that is to be connected with a three-dimensional, fluid-based description of the electrons [28].

Recent progress has focused on detailed and numerically efficient modelling of electron dynamics. Mahalingam and Menart [29] describe application of their numerical tools to investigate the performance of different magnetic field topologies in confining electrons. The same authors present a comprehensive assessment of their computational techniques by comparison of numerical and experimental results for the NASA NSTAR ion thruster [30], that was used on Deep Space-1. While the computed ion beam current

agrees with experiments within 1%, the computed discharge current differs from the measurements by more than 20%. Recently, a fully kinetic approach (PIC-MCC) has been presented by Mahalingham et al. [31] for computation of the electric field in an ion thruster discharge chamber. As with other thruster technologies, the computational models developed for meso-scale devices are also being applied to understand the plasma processes in smaller scale systems [32].

3.3.2 Cathodes

Two hollow cathodes are employed in a typical ion thruster system. One cathode is located inside the discharge chamber and provides the source of ionizing electrons. The second cathode is located external to the thruster and provides a source of electrons to neutralize the ion beam exiting the thruster. In general, there is interest in modelling these cathodes as their erosion is an important life-limiting mechanism for ion thrusters.

Due to the relatively high number density (10^{22} m^{-3}) and small physical size (1 cm) of a hollow cathode, much of the internal flow lies in the continuum regime. Rapid plume expansion, however, soon takes the flow into the kinetic regime. Relatively little research has been conducted on the development of numerical models of cathodes. Application of a conventional computational fluid dynamics model of the flow inside a hollow cathode was described by Murray et al. [33] that omitted much of the important plasma physics. A detailed one-dimensional model of the plasma flow inside a hollow cathode was described by Katz et al. [34]. Significant efforts have been made by Mikellides et al. [35, 36] to develop a detailed model of the plasma flow inside the hollow cathode and in the near-field plume expansion region near the keeper. A multi-fluid continuum approach is employed and assessed in detail through comparisons with experimental measurements for the NSTAR thruster [37]. An important conclusion from this work is a requirement for further theoretical investigations on the role of plasma turbulence in affecting cathode erosion. Another concern with cathodes is the depletion of the insert material as this reduces the ability of the device to generate electrons. An axisymmetric numerical model of the depletion process in a barium oxide cathode is described by Coletti and Gabriel [38] and assessed through direct comparisons with measurements obtained for several different cathodes [39].

3.3.3 Ion Optics

A large number of computer models for ion thruster ion optics performance have been developed over the years. Most of these models rely on the Particle in Cell (PIC) approach for simulating the rarefied plasma conditions. In addition, almost all of these codes consider the plasma flow through a single aperture of the grids due to the geometric complexity associated with a real thruster; for example, the NSTAR thruster has about 15,000 apertures.

Arakawa and Ishihara [23] combined their discharge model with a grid ion optics model based on Poisson's equation, the continuity equation, and Newton's 2nd law. Instead of using the PIC technique, a flux tube approach was adopted. A key omission from that model is the effect of charge exchange collisions. These interactions involve an electron being transferred from a slow neutral atom to a fast ion. The resulting low energy ions are very responsive to the electrostatic fields in the intergrid region, and it is these ions that are most likely to impinge on the grids causing sputtering and erosion. Peng et al. [40] describe a detailed simulation scheme employing the PIC technique and a Monte Carlo approach for simulating the charge exchange events. Further, the energy distribution of ions impinging on the grids was collected during the simulation and used to predict the erosion depths on the grid surface for 1000 hours of thruster operation. Bond and Latham [41] report on the use of a PIC code to modify the optics of the UK-10 ion thruster, that employs a three-grid configuration in which a third, *deceleration* grid is added. Good agreement was obtained between experimental measurements and the code predictions for the total current collected on the *acceleration* and *deceleration* grids at a number of different thruster operating conditions. The code was

subsequently employed to identify a modified grid geometry that would provide extended thruster lifetime. This was achieved through a combination of a smaller diameter for the *acceleration* grid holes and a thicker acceleration grid. In this way, the predicted lifetime was increased by almost a factor of two.

Later numerical simulation studies of ion optics continued to refine and develop these techniques in different ways. For example, Boyd and Crofton [42] introduced multiply charged ions and modelled collisions in detail using the DSMC technique. A typical computational domain is shown in Fig. 9. The plasma from the discharge chamber enters the flow domain along the left hand edge, labeled (1). The ions flow through the three-grid system of this thruster, biased at the voltages indicated, and exit the flow domain in the downstream plume region, labeled (2). In their study, Boyd and Crofton [42] considered several thruster operating conditions of the UK-10 thruster, and excellent agreement with measurements was obtained for *acceleration* grid current as shown in Fig. 10. Nakayama and Wilbur [43] describe a simplified grid optics analysis approach that allows thousands of parametric studies to be performed in just a few hours. Wang et al. [44] described a three-dimensional code that was applied to model erosion on the NSTAR thruster. In their work, it was realized that relatively long computational domains downstream of the *acceleration* grid are required in order to capture all of the back-flowing charge exchange ions. Figure 11 shows a comparison of the model with data obtained in an 8,200 hour life-test of the thruster. The code is remarkably successful in predicting the pits-and-grooves erosion patterns measured experimentally on the downstream face of the *acceleration* grid. The level of agreement is shown quantitatively in Fig. 12, where the erosion profiles on the grid are compared along a line joining two adjacent apertures.

Analysis of a single aperture of grid optics can be considered as one of the most mature areas of numerical simulation within electric propulsion. However, there remains the important question of how to integrate the results for one aperture across the entire grid face. This is not a straightforward procedure, as the discharge chamber usually creates some variation in ion current density across the screen grid while the profile of neutral atom properties tends to be much more uniform. These issues have been studied in detail by Emhoff and Boyd [45] for the NEXT ion thruster, in use on NASA's DAWN mission. The approach followed in [45] was to perform several simulations representing conditions corresponding to several different apertures across the thruster. The results from these simulations were then integrated across the thruster face to obtain overall performance data. In the case of the NEXT thruster, this approach yielded good agreement within 2% of measurements of thrust, specific impulse, and beam current [45]. In general, the accuracy of simulations associated with ion thruster optics is high in terms of propulsion performance, which explains why modelling now plays a key role in the development of this technology. Accurate simulation of lifetime related properties such as *acceleration grid* current and erosion is more problematic and requires continued research.

3.4 Hall Thrusters

A Hall thruster is essentially a grid-less electrostatic acceleration device that operates by flowing gas propellant (usually xenon or krypton) through holes in an anode into an annular acceleration channel. Electrons are supplied by an external hollow cathode. An applied magnetic field with a primarily radial component is used to partially trap the electrons in a desired region of the acceleration channel leading to a concentrated ionization zone. There are two main configurations of Hall thrusters. The so-called stationary plasma thruster (SPT) employs a relatively long acceleration channel (of a few centimeters) and ceramic wall insulator materials (e.g. boron nitride or silicon carbide). The anode layer thruster (TAL) employs a shorter acceleration channel (a few millimeters) and metallic wall materials (e.g. molybdenum). A schematic diagram of an SPT Hall thruster is provided in Fig. 13 that shows the main components. Typically, for both SPT's and TAL's, a potential difference between anode and cathode of several hundred volts is applied to accelerate the ions out of the annular channel. Specific impulses in the range of 1500 to 2500 seconds are achieved at an

overall efficiency of about 50-60%. The thrust level and specific impulse make Hall thrusters ideal for station-keeping tasks on communications spacecraft. As of May 2010, there were about 18 operational spacecraft using Hall thrusters in space. Notable applications of Hall thrusters include the SMART-1 mission (ESA) and many Russian communications satellites. The number of Hall thrusters operating in space will increase significantly in the next few years as commercial companies in the US and Europe have already begun implementing Hall thrusters on communications satellites for station-keeping.

There are several aspects of Hall thruster performance where numerical modelling can play a role in identifying improved operating conditions. Two of the key performance loss mechanisms involve collisions of ions with the walls of the acceleration channel, and beam divergence (see discussions in Kim [46]). Ions colliding with the walls lose their momentum and are reflected as slow neutral atoms. In order to contribute to thrust, these particles must be ionized and accelerated again, and this clearly represents a performance loss. In addition, the ions can impact the thruster walls at energies that are sufficiently large to sputter the wall material, and this represents one of the primary lifetime-limiting mechanisms of Hall thrusters. The divergence angle of the plume of a Hall thruster is significantly larger than that for a gridded ion thruster that leads to greater concerns over spacecraft integration as well as greater thrust loss. The main reasons for the increased plume divergence are the topology of the magnetic field that leaks out into the near-field plume region, and the larger electron temperature in a Hall thruster that leads to increased expansion of the plume.

The SPT-100 Hall thruster, developed in the former Soviet Union, produces a plasma density of about 10^{17} m^{-3} and a velocity of about 16 km/s in an acceleration channel with an annular diameter of 100 mm. The peak magnetic field strength is about 200 G; that means the electrons are magnetized and the ions are not. These physical characteristics indicate that while the electrons may be modelled using a fluid, continuum approach, the ions and neutrals require a kinetic formulation.

Almost all numerical modelling studies of Hall thrusters have considered the SPT configuration. One of the first investigations, by Komurasaki and Arakawa [47], employed a steady, two-dimensional formulation using a fluid electron model and a flux-tube ion model (similar to that used in ion thruster modeling). This approach was used to investigate basic plasma behaviour and thruster performance including ion loss to the walls. There are several important limitations in the approach of [47] including the omission of the neutrals and the assumption of steady state behaviour. Experimental measurements of Hall thrusters have detected a variety of oscillations including some in the range of 10-50 kHz that may play an important role in overall device performance. Such oscillations were predicted numerically in the one-dimensional, unsteady study of Boeuf and Garrigues [48] in which ions were modelled using the kinetic Vlasov equation, and the neutrals were included using a constant velocity and the continuity equation. A key limitation of this model is a phenomenological treatment of wall effects. A related one-dimensional model in which the ions were modelled using a PIC approach was described by Garrigues et al. [49], in which good qualitative agreement was obtained with experimental data for SPT performance characteristics for both xenon and krypton propellants, as shown in Fig. 14. Several alternative one-dimensional Hall thruster models have been successfully developed to explore fundamental properties of Hall thrusters. For example, Fruchtman et al. [50] used a fully fluid description to investigate the idea of controlling the electric field within the acceleration channel using absorbing electrodes, and Ahedo et al. [51] employed a three-fluid description (electrons, ions, and neutrals) to investigate effects of electron pressure and back-flow of ions to the anode. Similar formulations have been used to study other physical phenomena such as secondary electron emission from the walls [52] and two-stage Hall thrusters [53].

A variety of two-dimensional, unsteady Hall thruster models have also been developed. Fife and Martinez-Sanchez [54] used a self-consistent PIC model for ions and a quasi-one-dimensional fluid model for electrons.

A key aspect of this approach is to sub-cycle in time on the electron properties and thus the model is numerically expensive. This same model was used by Fife et al. [55] to perform a detailed analysis of the plasma-wall interaction phenomena and included the first numerical predictions of the plasma oscillations also computed by Boeuf and Garrigues [48]. A similar two-dimensional model was reported by Koo and Boyd [56] and applied to the AFRL/UM-P5 Hall thruster. Figure 15 illustrates a typical computational domain for these models in which the active simulation region lies between a virtual anode located inside the thruster and a virtual cathode located outside the thruster in the near-field plume region. In a sequence of investigations, Boeuf et al. [57,58,59,60] developed and extended the formulation of Fife, and used their model to investigate a number of phenomena including the role of electron mobility on the computational results, the effects of the magnetic field on thruster performance, and analysis of a two-stage Hall thruster. The models reported in [54-60] represent the state of the art in modelling Hall thruster performance. The accuracy of these models is found to depend heavily on the manner in which electron mobility is treated. It is found experimentally that the electron current obtained in the operation of Hall thrusters is higher than would be expected from classical modeling of electron mobility based on collisions between atoms and electrons. Attempts have been made to explain the enhanced mobility through electron collisions with the walls of the thruster (called near-wall conductivity), and by plasma oscillations or turbulence (called Bohm mobility). Near-wall conductivity has been analyzed in detail by Latocha et al. [61]. Using a fully kinetic, two-dimensional approach, Adam et al. [62] show that plasma turbulence may be generated under the high ion-velocity conditions at the exit of a Hall thruster and that such turbulence can lead to enhanced electron mobility. Despite these efforts, no general mobility model has yet been formulated to explain all the phenomena observed in thruster operation, and the issue of effective electron mobility modelling remains a critical area of on-going research for Hall thruster simulations. The current status is illustrated by Fig. 16 that shows profiles of plasma potential along the center of the annular acceleration channel of the UM/AFRL P5 Hall thruster [56]. It is found that the experimental data lies between the two simulations that employ models for Bohm mobility and wall-collision mobility.

The hybrid code developed by Fife and Martinez-Sanchez [54] is called HPHall, and this code has served as the basis for continued model development. The most recent version of the code, called HPHall2, has been advanced significantly by Hofer et al. [63,64,65]. In Ref. 63, new models for propellant injection and thruster wall reflections were found to improve agreement of computed results with experimental measurements. In Ref. 64, the wall sheath model of Hobbs and Wesson [66] was implemented and again found to improve the code predictions. Finally, a multiple-domain electron mobility model is introduced in Ref. 65 and found to offer the modeller increased control over this important phenomenon.

Efforts are continuing to develop more generalized approaches for modelling of the electrons in Hall thrusters. A shear-based model for electron transport was described by Scharfe et al. [67] but found to give agreement within no better than 30% with experimental measurements of thruster performance. A fully two-dimensional model for the electron dynamics was formulated by Escobar and Ahedo [68]. Despite the lack of a first principles electron mobility model, once a phenomenological model has been tuned for a particular type of thruster, numerical simulations can play a role in helping to better understand the complex, coupled plasma physics mechanisms present in Hall thrusters. For example, Scharfe et al. [69] use measurements of various thruster flow quantities to assess their numerical model and employ it to study effects of charge exchange and wall collisions. In two related studies, a tuned hybrid Hall thruster model was employed to investigate the potential benefits of a two-stage device in which the ionization and acceleration processes are physically separated [70,71].

A two-dimensional, steady, multi-fluid formulation has been developed for Hall thrusters by Keidar et al. [72]. These simulations require run times of minutes rather than the many hours required by the unsteady, hybrid fluid-particle methods. The fully fluid methods are therefore well-suited to the rapid analysis of critical

physical phenomena such as sheaths [72] and magnetic mirror effects [73]. The rapid simulation times offered by fluid formulations also make them very well suited to the investigation of thruster lifetime issues. For example, the change in Hall thruster wall profiles and overall thruster performance over several thousand hours of operation of the SPT-100 Hall thruster were investigated by Yim et al. [74] using a multi-fluid, two-dimensional model. Profiles of the predicted time evolution of the eroded walls are shown in Fig. 17 to offer very good correspondence to the experimentally measured behaviour. Significantly more expensive erosion studies have also been conducted based on hybrid simulations of the discharge plasma [75,76].

A two-dimensional, unsteady, multi-fluid Hall thruster formulation is described by Mikellides et al. [77] that is based on methods employed for modelling ion thruster hollow cathodes [36,37]. This approach offers several advantages over the hybrid-PIC technique including a fully two-dimensional electron model, the ability to extend the flow domain well outside the thruster, and smooth results that are free from the statistical fluctuations inherent in particle simulations. The method has been applied by Mikellides et al. [78] to explain unexpectedly low erosion rates measured on a 5 kW-class Hall thruster. Of course, this approach still requires input of an electron mobility model and cannot capture all of the nonequilibrium effects experienced by the discharge ions.

Anode layer Hall thrusters have received considerably less attention in terms of both thruster development and numerical simulation. A multi-fluid model of a high-power bismuth TAL was developed by Keidar and Boyd [79]. The model provided good agreement with measured current-voltage characteristics and was later further developed for application to a two-stage TAL thruster [80]. Due to the relatively small size of the acceleration channel in a TAL device, it can be argued that a particle approach is required to model both the electrons and the ions.

A fully kinetic, two-dimensional model for analysis of a 50-W micro-TAL Hall thruster was formulated by Szabo and Martinez-Sanchez [81]. All physical phenomena were modeled on the electron time-scale. Certain non-physical assumptions had to be invoked to make the problem numerically tractable, such as increasing the electron-to-ion mass ratio, and increasing the permittivity of free space. Fully kinetic analyses of SPT-like thrusters have also been presented by Blateau et al. [82] and Irishkov et al. [83] employing similar simplifying assumptions. In both Refs. 82 and 83, the simulations over predict the measured thrust by about 10% and the efficiency by about 50%. Clearly, there is still significant progress required to improve various aspects of fully kinetic simulation of Hall thrusters. Nevertheless, this is a likely direction for future research as computer power continues to increase, allowing more accurate simulation of the electron dynamics.

Due primarily to uncertainties in electron mobility modelling, both fluid and hybrid simulations schemes are generally only capable of predicting Hall thruster performance (thrust and power) within about 10%. However, once a simulation method has been tuned using a phenomenological mobility model, better accuracy can be expected over a limited range of thruster operating conditions.

4.0 SUMMARY

The successful development of physically accurate numerical methods for simulating the gas and plasma flows in electric propulsion thrusters has the potential to significantly improve the design process of these devices. This goal has been partially realized with numerical simulations playing an increasing role in the design, particularly of ion thrusters and Hall thrusters. Nevertheless, the accurate simulation of many electric propulsion thrusters remains a significant challenge due to the difficulties associated with the need to model the wide variety of physical phenomena that occur in these systems, including viscous gas dynamics,

nonequilibrium collisions, rarefied plasma physics, and surface interactions. In terms of predicting thruster performance, accuracy of the existing numerical methods ranges from within 5% for resisto-jets and ion thrusters, to within 10- 20% for arcjets and Hall thrusters.

There are two main directions for future work to continue to improve the numerical modelling of electric thrusters. First, the numerical methods themselves must be improved in terms of their physical accuracy and their computational speed. The level of physical accuracy required in the modelling of a particular thruster depends on the nature of the acceleration mechanism employed. To make valuable contributions to the design process, computational analyses are most useful when they predict the correct trends in solution times of a few hours. This latter aspect is in part addressed automatically by the continued increase in computational power provided by hardware and software developments. The second main direction for improvement in the simulations involves the more accurate determination of physical parameters that are required by the numerical formulations. Examples of such information include sputter yields for new grid materials that might be used in gridded ion thrusters, secondary electron coefficients of wall materials used in Hall thrusters, electron mobility and other transport coefficients, and cross sections for new propellant species. These data are most likely to be obtained computationally due to the development of molecular dynamics simulation methods, and the expense and difficulty of performing laboratory experiments to measure such data.

5.0 ACKNOWLEDGMENT

The author gratefully acknowledges funding provided to support this work by the Air Force Research Laboratory (AFRL) through the Michigan/AFRL Center of Excellence in Electric Propulsion (grant F9550-09-1-0695).

6.0 REFERENCES

- [1] Tannehill, J.C., Anderson, D.A., and Pletcher, R.H., *Computational Fluid Mechanics and Heat Transfer*, Taylor and Francis, 1997.
- [2] Fletcher, C.A.J., *Computational Techniques for Fluid Dynamics*, Vols. I and II, Springer-Verlag, Berlin, 1991.
- [3] Bird G.A., *Molecular Gas Dynamics and the Direct Simulation of Gas Flows*, Oxford University Press, 1994.
- [4] Birdsall C.K., "Particle-in-cell charged particle simulations, plus Monte Carlo collisions with neutral atoms, PIC-MCC," *IEEE Transactions on Plasma Science*, Vol. 19, 1991, pp. 65-85.
- [5] Birdsall, C.K. and Langdon, A.B., *Plasma Physics Via Computer Simulation*, Adam Hilger Press, 1991.
- [6] Kim, S.C., "Calculations of Low-Reynolds-Number Resistojet Nozzles," *Journal of Spacecraft and Rockets*, Vol. 31, 1994; pp. 259-264.
- [7] Boyd, I.D., Penko, P.F., Meissner, D.L., and DeWitt, K.J., "Experimental and Numerical Investigations of Low-Density Nozzle and Plume Flows of Nitrogen," *AIAA Journal*, Vol. 30 (10), 1992, pp. 2453-2461.

Simulation of Electric Propulsion Thrusters

- [8] Boyd, I.D., VanGilder, D.B., and Beiting, E.J., “Numerical and Experimental Investigations of Rarefied Flow in a Small Nozzle,” *AIAA Journal*, Vol. 34, 1996, pp. 2320-2326.
- [9] Ahmed, Z., Gimelshein, S.F., and Ketsdever, A.D., “Numerical Analysis of Free-Molecule Microresistojet Performance,” *Journal of Propulsion and Power*, Vol. 22 (4), 2006, pp. 749-756.
- [10] Gibbon, D., Coxhill, I., Nicolini, D., Correia, R., and Page, J., “The Design, Development and In-flight Operation of a Water Resistojet Micropropulsion System,” AIAA Paper No. 2004-3798, July 2004.
- [11] Coxhill, I. and Gibbon, D., “A Xenon Resistojet Propulsion System for Microsatellites,” AIAA Paper No. 2005-4260, July 2005.
- [12] Robin, M., Brogan, T., and Cardiff, E., “An Ammonia Microresistojet (MRJ) for Micro Satellites,” AIAA Paper 2008-5288, July 2008.
- [13] Butler, G.W. and King, D.Q., “Single and Two Fluid Simulations of Arcjet Performance,” AIAA Paper No. 92-3104, July 1992.
- [14] Miller, S.A. and Martinez-Sanchez, M., “Two-Fluid Nonequilibrium Simulation of Hydrogen Arcjet Thrusters,” *Journal of Propulsion and Power*, Vol. 12, 1996, pp. 112-119.
- [15] Megli, T.W., Krier, H., and Burton, R.L., “Plasmadynamics Model for Nonequilibrium Processes in N_2H_2 Arcjets,” *Journal of Thermophysics and Heat Transfer*, Vol. 10, 1996, pp. 554-562.
- [16] Auweter-Kurtz, M., Goelz, T., Habiger, H., Hammer, F., Kurtz, H., Riehle, M., and Sleziona, C., “High-Power Hydrogen Arcjet Thrusters,” *Journal of Propulsion and Power*, Vol. 14, 1998, pp. 764-773.
- [17] Boyd, I.D., “Monte Carlo Simulation of Nonequilibrium Flow in Low Power Hydrogen Arcjets,” *Physics of Fluids*, Vol. 9, 1997, pp. 3086-3095.
- [18] Boyd, I.D., “Extensive Validation of a Monte Carlo Model for Hydrogen Arcjet Flow Fields,” *Journal of Propulsion and Power*, Vol. 13, 1997, pp. 775-782.
- [19] Hatta, S. and Aso, S., “Numerical Studies on Effect of Nozzle Geometry and of Flow Continuity on Thrust Performance,” Paper 01-193, 27th International Electric Propulsion Conference, September 2001.
- [20] Laure, S., Heiermann, J., Auweter-Kurtz, M., and Kurtz, H., “Experimental and Numerical Investigation of a Power Augmented Thermal Arc Jet,” AIAA Paper No. 2001-3923, July 2001.
- [21] Bock, D., Auweter-Kurtz, M., and Kurtz, H., “1 kW Ammonia Arcjet System Development for a Science Mission to the Moon,” Paper 05-075, 29th International Electric Propulsion Conference, March 2005.
- [22] Slough, J. and Ewing, J.J., “Microarcjet Microthruster for Nanosat Applications,” AIAA Paper 2007-5181, July 2007.
- [23] Arakawa, Y. and Ishihara, K., “A Numerical Code for Cusped Ion Thrusters,” Paper 91-118, 22nd International Electric Propulsion Conference, 1991.

- [24] Jugroot, M. and Harvey, J.K., "Numerical Modeling of Neutral and Charged Particles Within a Gridded Ion Thruster," Paper 01-100, 27th International Electric Propulsion Conference, September 2001.
- [25] Wirz, R. and Katz, I., "2-D Discharge Chamber Model for Ion Thrusters," AIAA Paper No. 2004-4107, July 2004.
- [26] Mahalingam, S. and Menart, J., "Computational Model Tracking Primary Electrons, Secondary Electrons and Ions in the Discharge Chamber of an Ion Engine," AIAA Paper No. 2005-4253, July 2005.
- [27] Stueber, T., "Ion Thruster Discharge Chamber Simulation in Three Dimensions," AIAA Paper No. 2005-3688, July 2005.
- [28] Stueber, T., "Discharge Chamber Primary Electron Modeling Activities in 3-Dimensions," AIAA Paper No. 2004-4105, July 2004.
- [29] Mahalingam, S. and Menart, J., "Computational Study of Primary Electron Confinement by Magnetic Fields in the Discharge Chamber of an Ion Engine," *Journal of Propulsion and Power*, Vol. 23, 2007, pp. 69-72.
- [30] Mahalingam, S. and Menart, J., "Particle Based Plasma Simulation for an Ion Engine Discharge Chamber," *Journal of Propulsion and Power*, Vol. 26, 2010, pp. 673-688.
- [31] Mahalingam, S., Choi, Y., Loverich, J., Stoltz, P.H., Jonell, M., and Menart, J., "Dynamic Electric Field Calculations Using a Fully Kinetic Ion Thruster Discharge Chamber Model," AIAA Paper 2010-6944, July 2010.
- [32] Wirz, R., "Computational Modeling of a Miniature Ion Thruster Discharge," AIAA Paper 2005-3887, July 2005.
- [33] Murray, D.M., Tutty, O.R., and Gabriel, S.B., "Numerical Modelling of Ion Thruster Hollow Cathode Interior Flow," AIAA Paper No. 1997-793, January 1997.
- [34] Katz, I., Anderson, J.R., Polk, J.E., and Brophy, J.R., "One-Dimensional Hollow Cathode Model," *Journal of Propulsion and Power*, Vol. 19, 2003, pp. 595-600.
- [35] Mikellides, I.G., Katz, I., Goebel, D., and Polk, J.E., "Theoretical Modeling of a Hollow Cathode Plasma for the Assessment of Insert and Keeper Lifetimes," AIAA Paper No. 2005-4234, July 2005.
- [36] Mikellides, I.G., Katz, I., and Goebel, D., "Numerical Simulation of the Hollow Cathode Discharge Plasma Dynamics," Paper 05-200, 29th International Electric Propulsion Conference, 2005.
- [37] Mikellides, I.G., Katz, I., Goebel, D., Jameson, K.K., and Polk, J.E., "Wear Mechanisms in Electron Sources for Ion Propulsion, 2: Discharge Hollow Cathode," *Journal of Propulsion and Power*, Vol. 24, 2008, pp. 866-879.
- [38] Coletti, M. and Gabriel, S.B., "A Model for Barium Oxide Depletion from Hollow Cathode Inserts: Modeling and Comparison With Experiments," *IEEE Transactions on Plasma Science*, Vol. 37, 2009, pp. 58-66.

- [39] Coletti, M. and Gabriel, S.B., “Barium Oxide Depletion from Hollow Cathode Inserts: Modeling and Comparison With Experiments,” *Journal of Propulsion and Power*, Vol. 26, 2010, pp. 364-369.
- [40] Peng, X., Keefer, D., and Ruyten, W.M., “Plasma Particle Simulation of Electrostatic Ion Thrusters,” *Journal of Propulsion and Power*, Vol. 8, 1992, pp. 361-366.
- [41] Bond, R.A. and Latham, P.M., “Ion Thruster Extraction Grid Design and Erosion Modeling Using Computer Simulation,” AIAA Paper No. 95-2923, July 1995.
- [42] Boyd, I.D. and Crofton, M.W., “Grid Erosion Analysis of the T5 Ion Thruster,” AIAA Paper No. 2001-3781, July 2001.
- [43] Nakayama, Y. and Wilbur, P.J., “Numerical Simulation of Ion Beam Optics for Many-Grid Systems,” AIAA Paper No. 2001-3782, July 2001.
- [44] Wang, J., Polk, J.E., Brophy, J.R., and Katz, I., “Three-Dimensional Particle Simulations of Ion-Optics Plasma Flow and Grid Erosion,” *Journal of Propulsion and Power*, Vol. 19, 2003, pp. 1192-1199.
- [45] Emhoff, J.W. and Boyd, I.D., “Modeling of Total Thruster Performance for NEXT Ion Optics,” *Journal of Propulsion and Power*, Vol. 22, 2005, pp. 741-748.
- [46] Kim, V., “Main Physical Features and Processes Determining the Performance of Stationary Plasma Thrusters,” *Journal of Propulsion and Power*, Vol. 14, 1998, pp. 736-743.
- [47] Komurasaki, K. and Arakawa, Y., “Two-Dimensional Numerical Model of Plasma Flow in a Hall Thruster,” *Journal of Propulsion and Power*, Vol. 11, 1995, pp. 1317-1323.
- [48] Boeuf, J.P. and Garrigues, L., “Low Frequency Oscillations in a Stationary Plasma Thruster,” *Journal of Applied Physics*, Vol. 84, 1998, pp. 3541-3554.
- [49] Garrigues, L., Boyd, I.D., and Boeuf, J.P., “Computation of Hall Thruster Performance,” *Journal of Propulsion and Power*, Vol. 17, 2001, pp. 772-779.
- [50] Fruchtman, A., Fisch, N.J., and Raites, Y., “Hall Thruster With Absorbing Electrodes,” AIAA Paper No. 2000-3659, July 2000.
- [51] Ahedo, E., Martinez-Cerezo, P., and Martinez-Sanchez, M., “One-Dimensional Model of the Plasma Flow in a Hall Thruster,” *Physics of Plasmas*, Vol. 8, 2001, pp. 3058-3068.
- [52] Ahedo, E. and Parra, F.I., “A model of the Two-Stage Hall Thruster Discharge,” *Journal of Applied Physics*, Vol. 98, 2005, article 023303.
- [53] Ahedo, E. and Parra, F.I., “Partial Trapping of Secondary-Electron Emission in a Hall Thruster Plasma,” *Physics of Plasmas*, Vol. 12, 2005, article 073503.
- [54] Fife, J.M. and Martinez-Sanchez, M., “Two-Dimensional Hybrid Particle In Cell Modeling of Hall Thrusters,” IEPC Paper 95-240, September 1995.
- [55] Fife, J.M., Martinez-Sanchez, M., and Szabo, J., “A Numerical Study of Low-Frequency Oscillations in

- Hall Thrusters,” AIAA Paper No. 97-3052, July 1997.
- [56] Koo, J. and Boyd, I.D., “Computational Model of a Hall Thruster,” *Computational Physics Communications*, Vol. 164, 2004, pp. 442-447.
- [57] Hagelaar, G.J.M., Bareilles, J., Garrigues, L., and Boeuf, J.P., “Two-Dimensional Model of a Stationary Plasma Thruster,” *Journal of Applied Physics*, Vol. 91, 2002, pp. 5592-5598.
- [58] Garrigues, L., Hagelaar, G.J.M., Bareilles, J., Boniface, C., and Boeuf, J.P., “Model Study of the Influence of the Magnetic Field Configuration on the Performance and Lifetime of a Hall Thruster,” *Physics of Plasmas*, Vol. 10, 2003, pp. 4886-4892.
- [59] Bareilles, J., Hagelaar, G.J.M., Garrigues, L., Boniface, C., Boeuf, J.P., and Gascon, N., “Critical Assessment of a Two-Dimensional Hybrid Hall Thruster Model: Comparisons With Experiments,” *Physics of Plasmas*, Vol. 11, 2004, pp. 3035-3046.
- [60] Boniface, C., Hagelaar, G.J.M., Garrigues, L., Boeuf, J.P., and Prioul, A., “Modeling of Double Stage Hall Effect Thruster,” *IEEE Transactions on Plasma Science*, Vol. 33, 2005, pp. 522-523.
- [61] Latocha, V., Garrigues, L., Degond, P., and Boeuf, J.P., “Numerical Simulation of Electron Transport in the Channel Region of a Stationary Plasma Thruster,” *Plasma Sources Science and Technology*, Vol. 11, 2002, pp. 104-114.
- [62] Adam, J.C., Heron, A., and Laval, G., “Study of Stationary Plasma Thrusters Using Two-Dimensional Fully Kinetic Simulations,” *Physics of Plasmas*, Vol. 11, 2004, pp. 295-305.
- [63] Hofer, R.R., Katz, I., Mikellides, I.G., and Gamero-Castano, M., “Heavy Particle Velocity and Electron Mobility Modeling in Hybrid-PIC Hall Thruster Simulations,” AIAA Paper 2006-4658, July 2006.
- [64] Hofer, R.R., Mikellides, I.G., Katz, I., and Goebel, D.M., “Wall Sheath and Electron Mobility Modeling in Hybrid-PIC Hall Thruster Simulations,” AIAA Paper 2007-5267, July 2007.
- [65] Hofer, R.R., Katz, I., Mikellides, I.G., Goebel, D.M., Jameson, K.K., Sullivan, R.M., and Johnson, L.K., “Efficacy of Electron Mobility Models in Hybrid-PIC Hall Thruster Simulations,” AIAA Paper 2008-4924, July 2008.
- [66] Hobbs, G. D. and Wesson, J. A., "Heat Flow through a Langmuir Sheath in the Presence of Electron Emission," *Plasma Physics*, Vol. 9, 1967, pp. 85-87.
- [67] Scharfe, M.K., Thomas, C.A., Scharfe, D.B., Gascon, N., Cappelli, M.A., and Fernandez, E., “Shear-Based Model for Electron Transport in Hybrid Hall Thruster Simulations,” *IEEE Transactions on Plasma Science*, Vol. 36, 2008, pp. 2058-2068.
- [68] Escobar, D. and Ahedo, E., “Two-Dimensional Electron Model for a Hybrid Code of a Two-Stage Hall Thruster,” *IEEE Transactions on Plasma Science*, Vol. 36, 2008, pp. 2043-2057.
- [69] Scharfe, M., Gascon, N., and Cappelli, M.A., “Comparison of Hybrid Hall Thruster Model to Experimental Measurements,” *Physics of Plasmas*, Vol. 13, 2006, Article 083505.

Simulation of Electric Propulsion Thrusters

- [70] Perez-Luna, J., Hagelaar, G.J.M., Garrigues, L., and Boeuf, J.P., "Model Analysis of a Double-Stage Hall Effect Thruster With Double-Peaked Magnetic Field and Intermediate Electrode," *Physics of Plasmas*, Vol. 14, 2007, Article 113502.
- [71] Garrigues, L., Boniface, C., Hagelaar, G.J.M., and Boeuf, J.P., "Modeling of an Advanced Concept of a Double Stage Hall Effect Thruster," *Physics of Plasmas*, Vol. 15, 2008, Article 113502.
- [72] Keidar, M., Boyd, I.D., and Beilis, I.I., "Plasma Flow and Plasma-Wall Transition in Hall Thruster Channel," *Physics of Plasmas*, Vol. 8, 2001, pp. 5315-5322.
- [73] Keidar, M. and Boyd, I.D., "On the Magnetic Mirror Effect in Hall Thrusters," *Applied Physics Letters*, Vol. 87, 2005, article 121501.
- [74] Yim, J.T., Keidar, M., and Boyd, I.D., "A Hydrodynamic-Based Erosion Model for Hall Thrusters," IEPC Paper 05-013, November 2005.
- [75] Sommier, E., Scharfe, M.K., Gascon, N., Cappelli, M.A., and Fernandez, E., "Simulating Plasma-Induced Hall Thruster Wall Erosion With a Two-Dimensional Hybrid Model," *IEEE Transactions on Plasma Science*, Vol. 35, 2007, pp. 1379-1387.
- [76] Cheng, S.Y. and Martinez-Sanchez, M., "Hybrid Particle-in-Cell Erosion Modeling of Two Hall Thrusters," *Journal of Propulsion and Power*, 2008, pp. 987-998.
- [77] Mikellides, I. G., and Katz, I., Hofer, R. R., Goebel, D. M., "Hall-Effect Thruster Simulations with 2-D Electron Transport and Hydrodynamic Ions," IEPC Paper 09-114, September 2009.
- [78] Mikellides, I.G., Katz, I., Hofer, R.R., Goebel, D.M., de Grys, K., and Mathers, A., "Magnetic Shielding of the Acceleration Channel Walls in a Long-Life Hall Thruster," AIAA Paper 2010-6942, July 2010.
- [79] Keidar, M., Boyd, I.D., and Beilis, I.I., "Modeling of a High-Power Thruster With Anode Layer," *Physics of Plasmas*, Vol. 11, 2004, pp. 1715-1722.
- [80] Keidar, M., Choi, Y., and Boyd, I.D., "Modeling of a Two-Stage High-Power Anode Layer Thruster and its Plume," *Journal of Propulsion and Power*, Vol. 23, 2007, pp. 500-506.
- [81] Szabo, J. and Martinez-Sanchez, M., "Fully Kinetic Hall Thruster Modeling," IEPC Paper 01-341, October 2001.
- [82] Blateau, V., Martinez-Sanchez, M., and Batischev, O., "A Computational Study of Internal Physics Effects in a Hall Thruster," AIAA Paper No. 2002-4105, July 1995.
- [83] Irishkov, S.V., Gorshkov, O.A., and Shagayda, A.A., "Fully Kinetic Modeling of Low-Power Hall Thrusters," IEPC Paper 05-035, November 2005.

Table 1. Properties of Various Electric Propulsion Thruster Types

Thruster	Thrust (mN)	Specific Impulse (sec)	Number Density (m⁻³)	Flow Regime
Resistojet	2-100	200-300	10 ²¹ -10 ²³	Continuum/Kinetic
Arcjet	2-700	400-1500	10 ²² -10 ²³	Continuum/Kinetic
Ion Thruster	0.01-200	1500-5000	10 ¹⁷ -10 ¹⁸	Kinetic
Hall Thruster	0.01-1000	1500-6000	10 ¹⁸ -10 ¹⁹	Kinetic

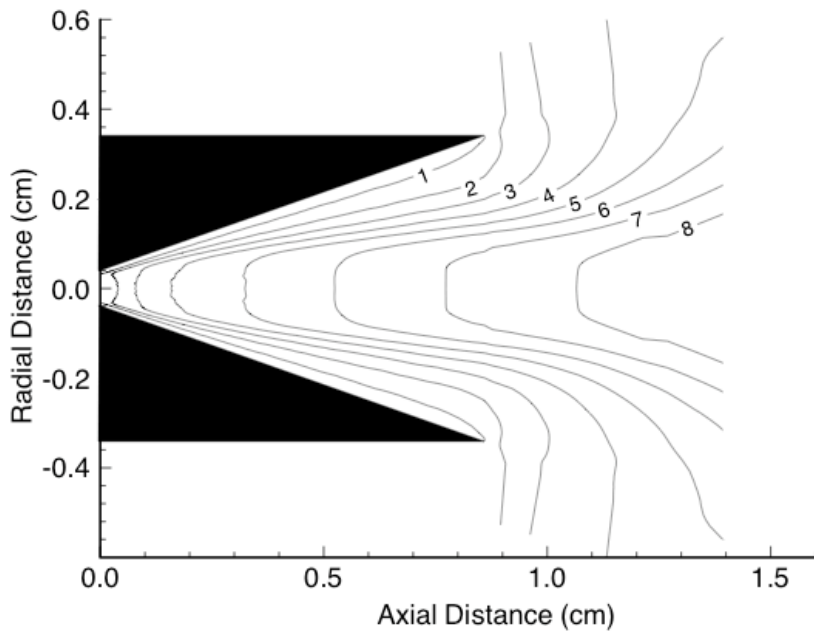


Figure 1. Mach number contours in a hydrogen resisto-jet (from Boyd et al. [8]).

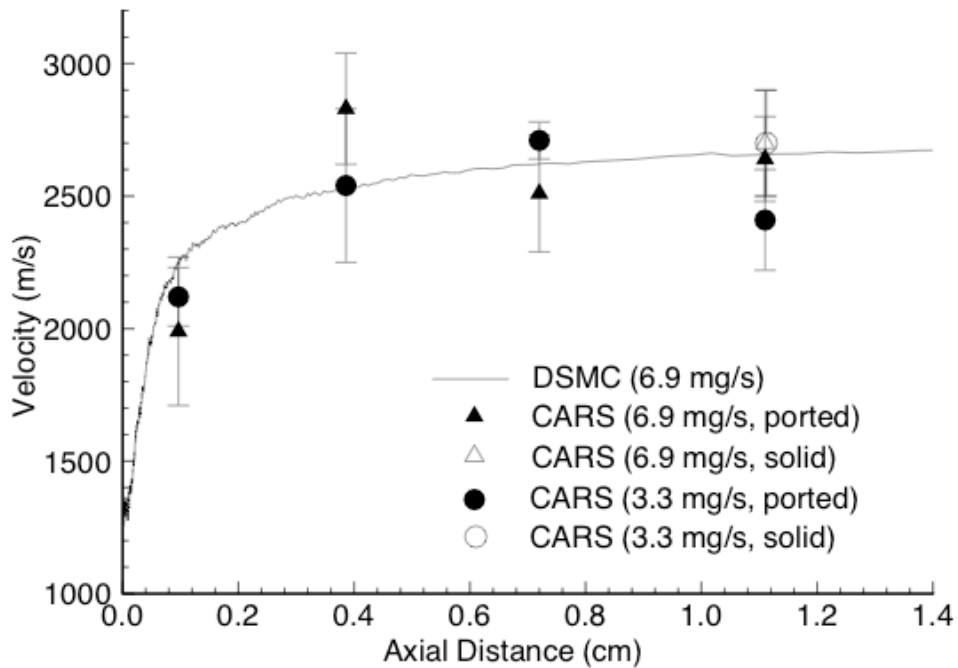


Figure 2. Axial velocity profiles for a hydrogen resisto-jet (from Boyd et al. [8]).

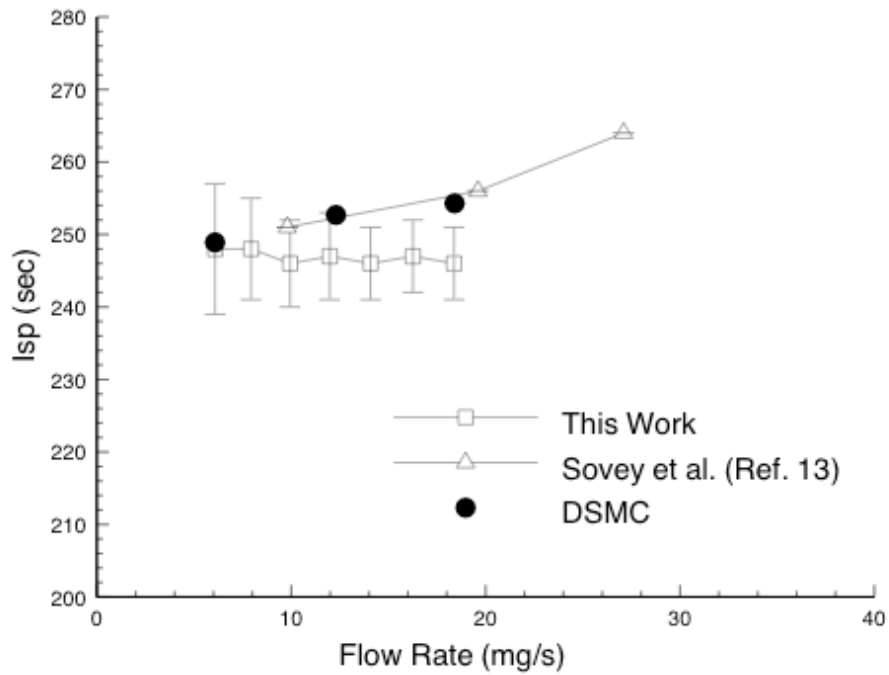


Figure 3. Specific impulse for a hydrogen resisto-jet (from Boyd et al. [8]).

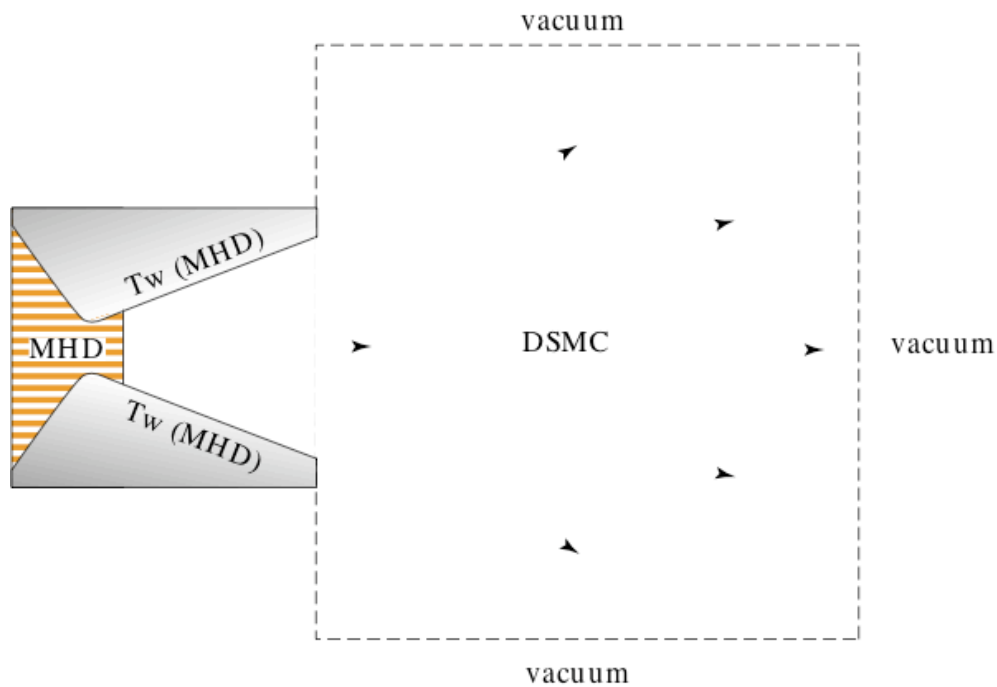


Figure 4. Schematic diagram illustrating DSMC arcjet analysis (from Boyd [18]).

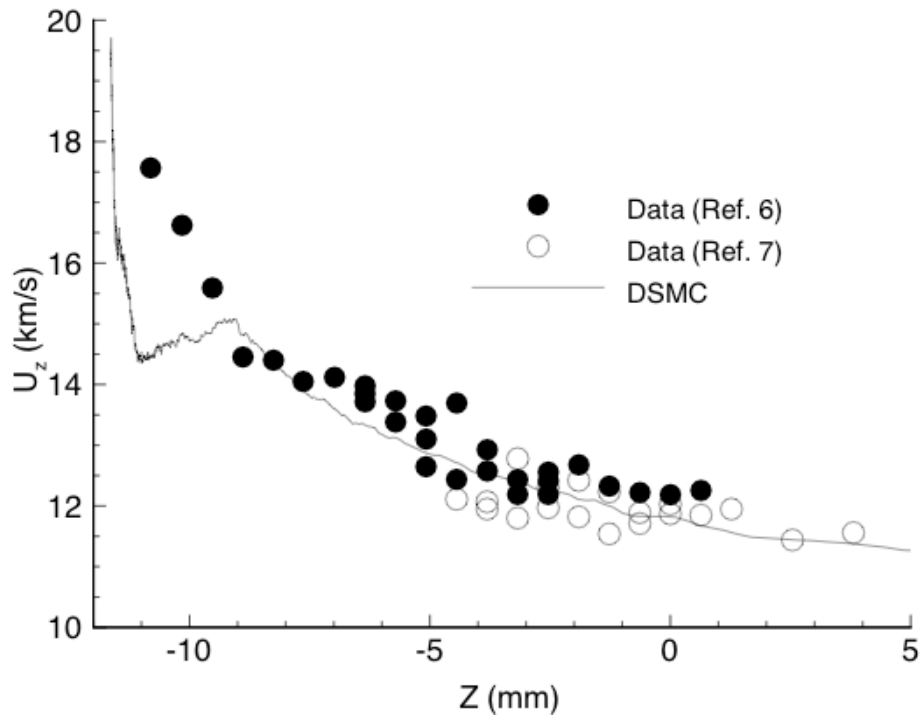


Figure 5. Axial velocity profiles in a hydrogen arcjet (from Boyd [18]).

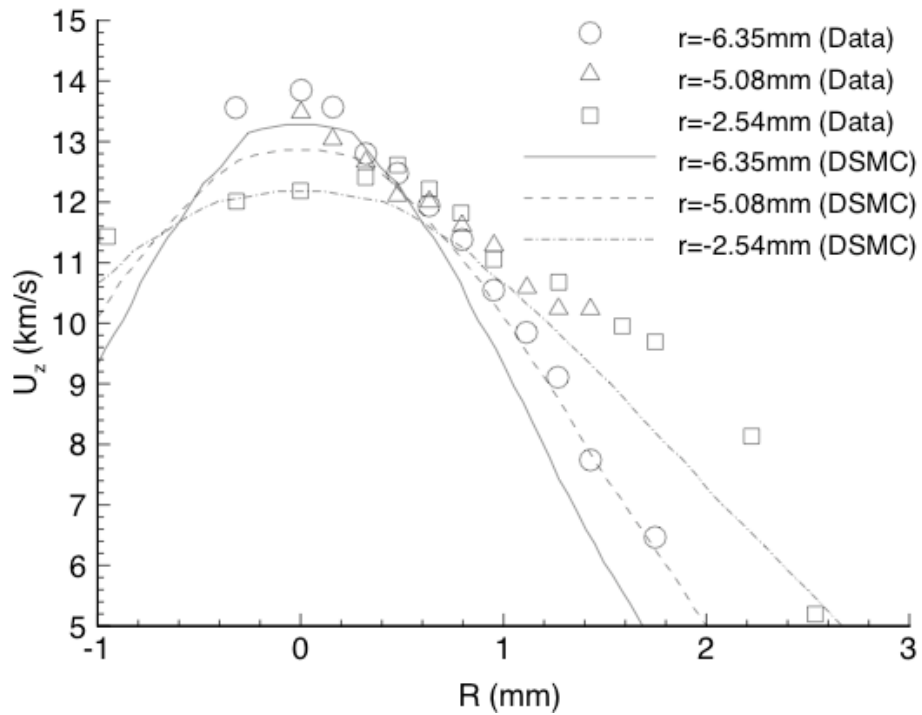


Figure 6. Radial velocity profiles in a hydrogen arcjet (from Boyd [18]).

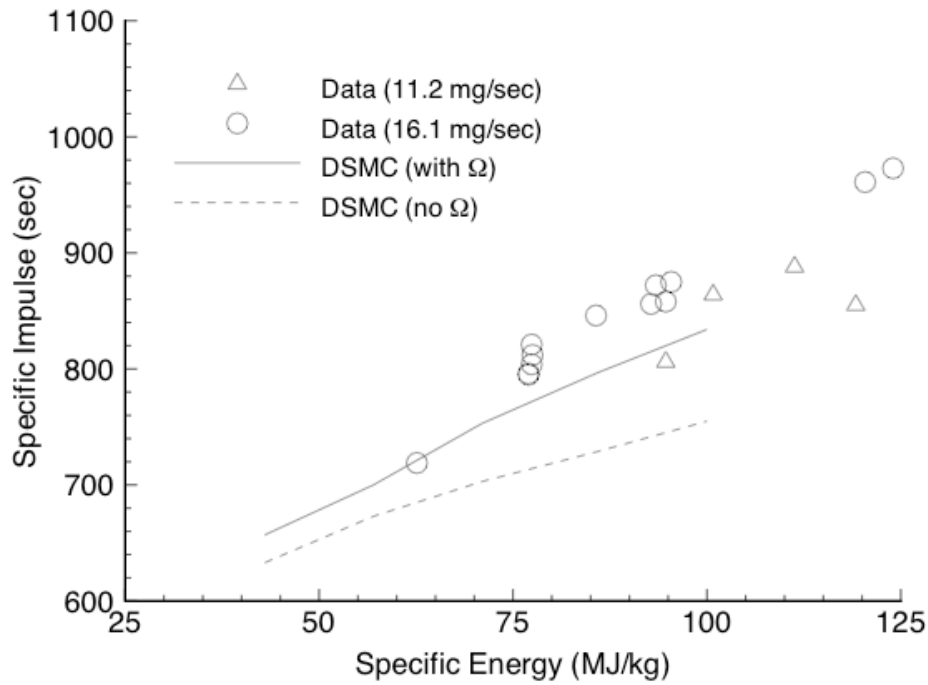


Figure 7. Specific impulse for a hydrogen arcjet (from Boyd [18]).

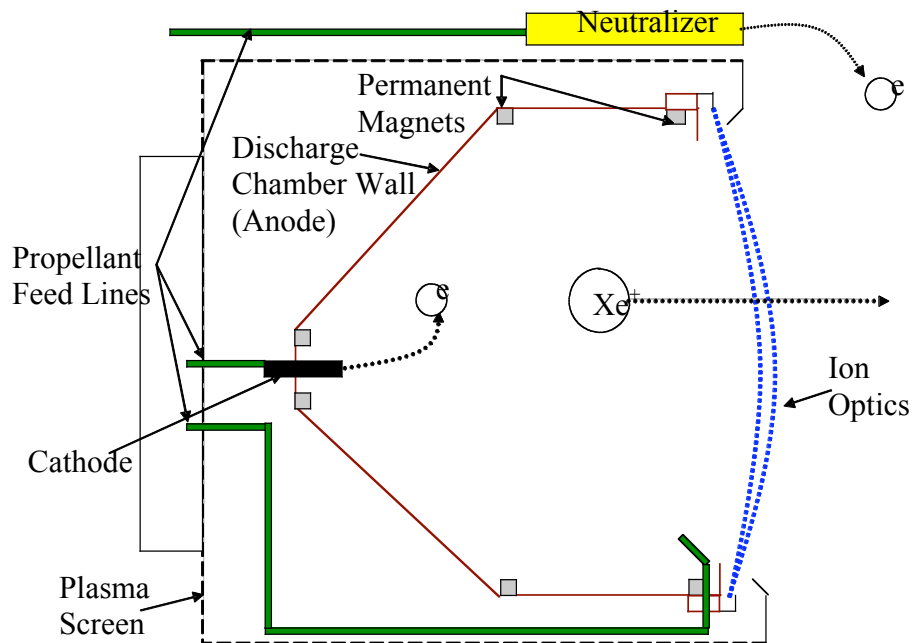


Figure 8. Schematic diagram of an ion thruster.

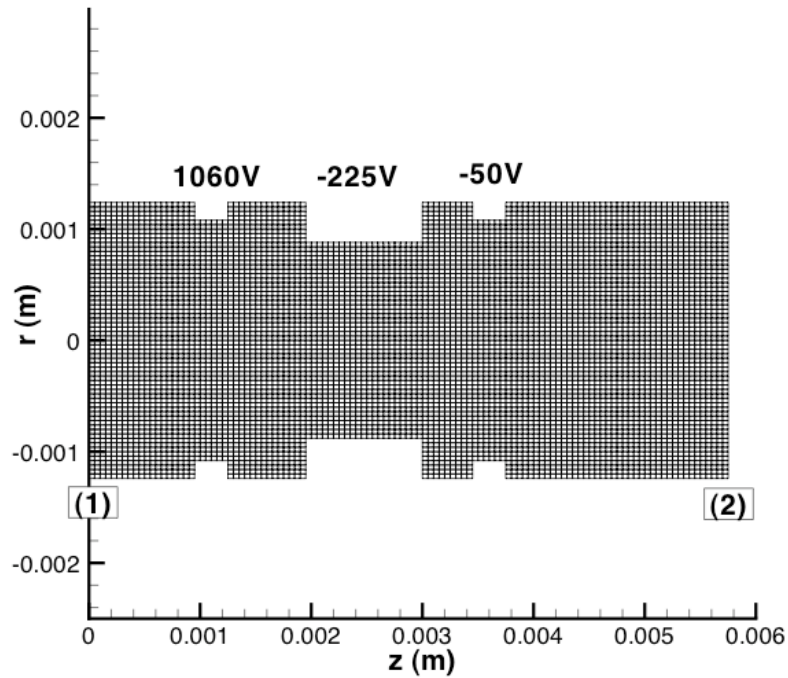


Figure 9. Computational domain for ion optics simulation (from Boyd and Crofton [42]).

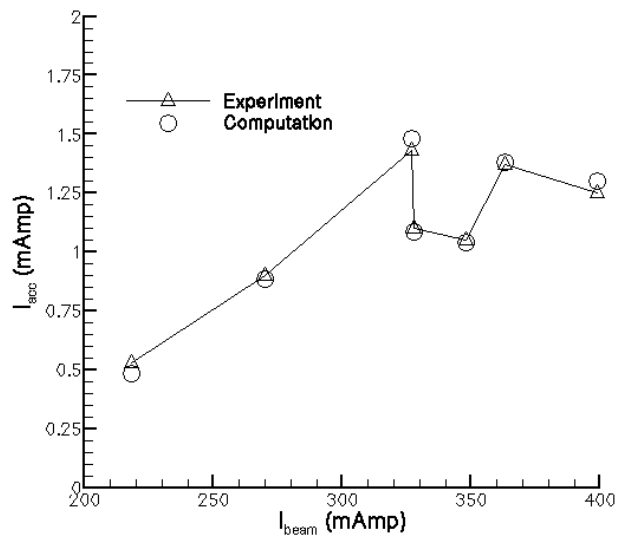


Figure 10. DSMC-PIC analysis of current collection on the *acceleration* grid of the UK-10 ion thruster (from Boyd and Crofton [42]).

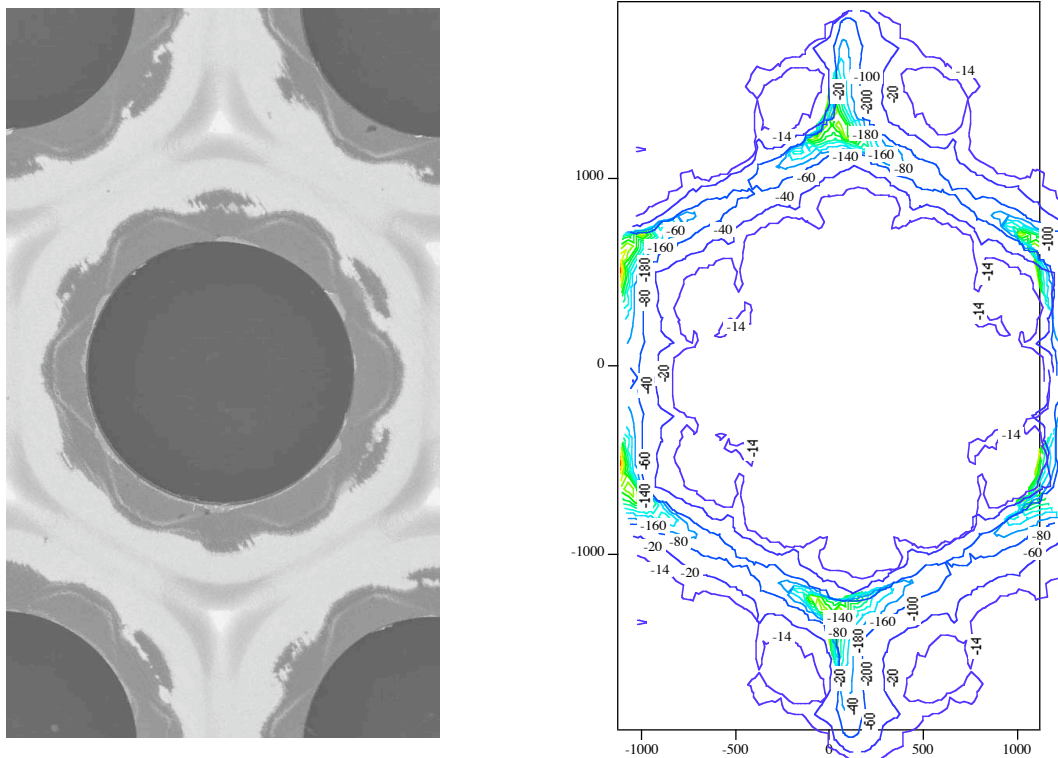


Figure 11. Erosion pattern around a single aperture on the downstream face of the *acceleration* grid of the NSTAR thruster: photograph (left) and simulation (right) (from Wang et al. [44]).

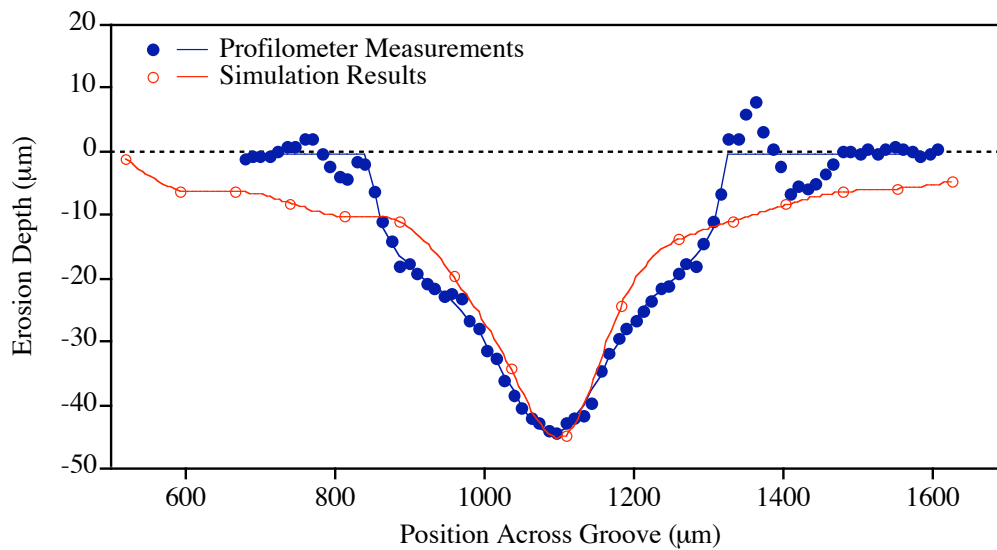


Figure 12. Erosion profile between the centers of two adjacent apertures for the *acceleration* grid of the NSTAR thruster (from Wang et al. [44]).

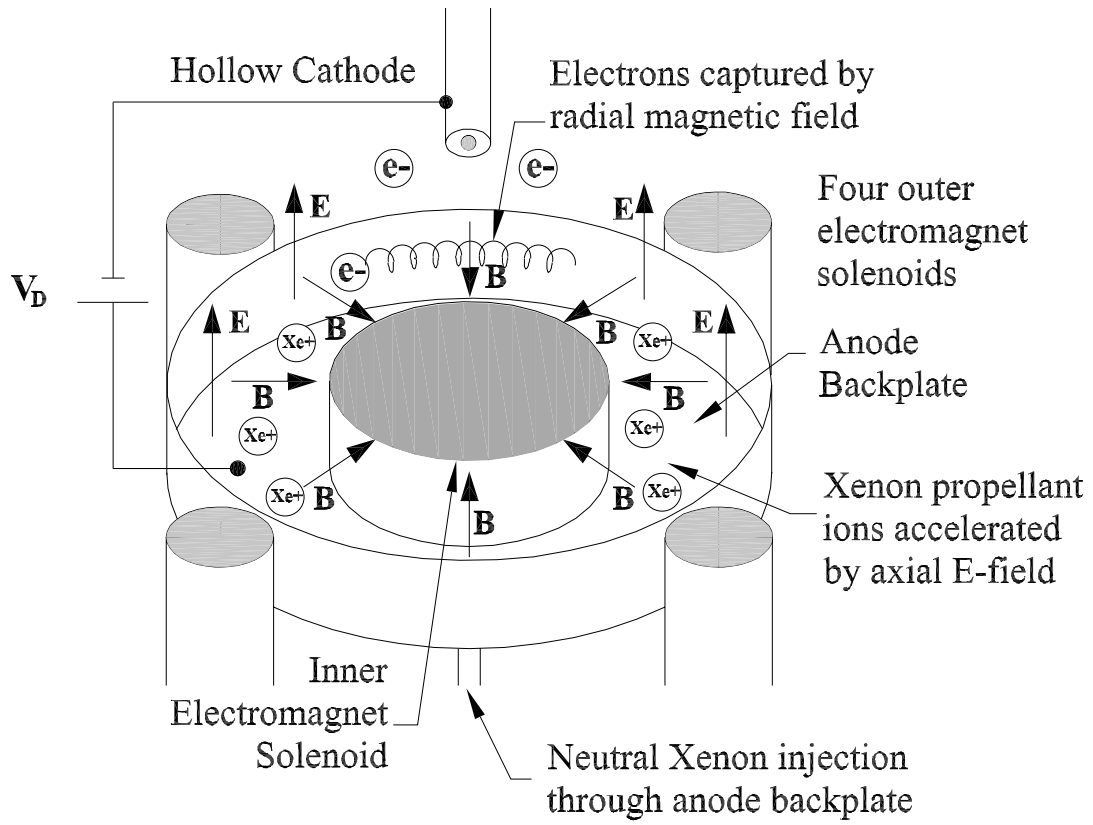


Figure 13. Schematic diagram of a Hall thruster.

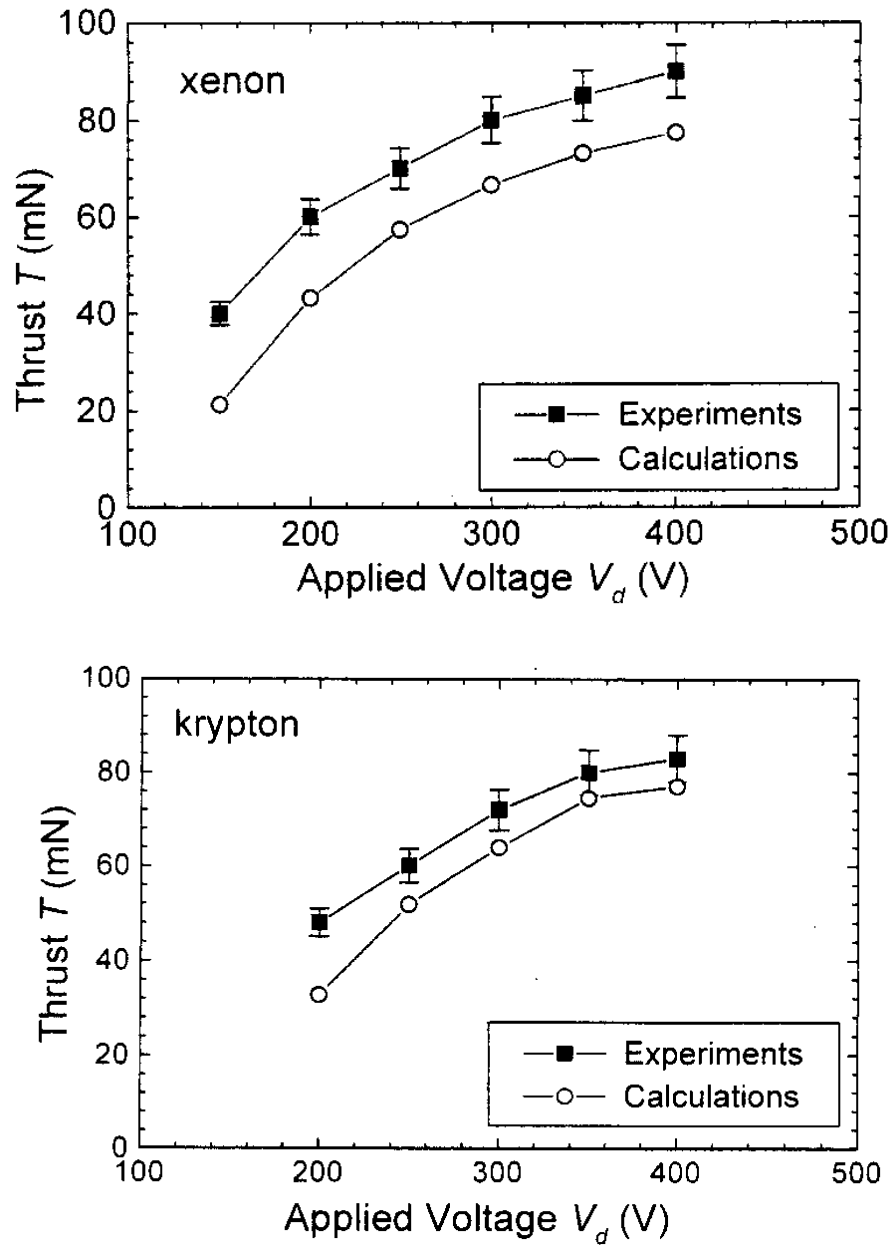


Figure 14. One-dimensional PIC analysis of the performance of an SPT Hall thruster using xenon and krypton propellants (from Garrigues et al. [49]).

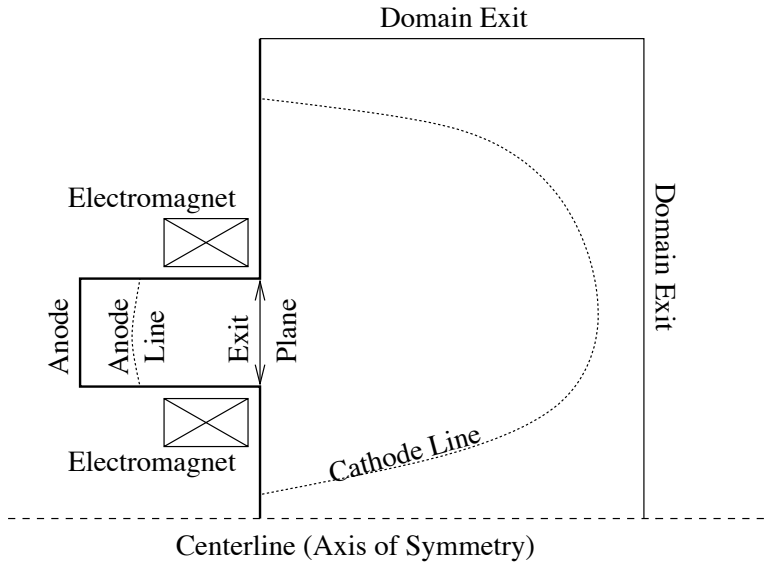


Figure 15. Computational domain for Hall thruster simulation.

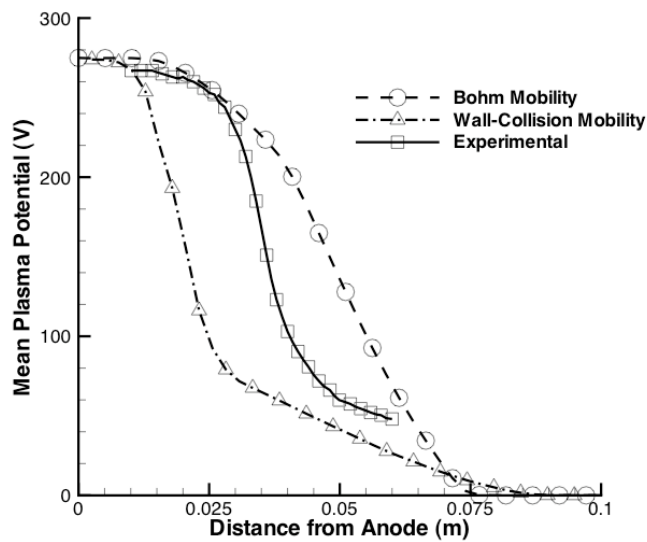


Figure 16. Centerline profiles of plasma potential for the P5 Hall thruster (from Koo and Boyd [56]).

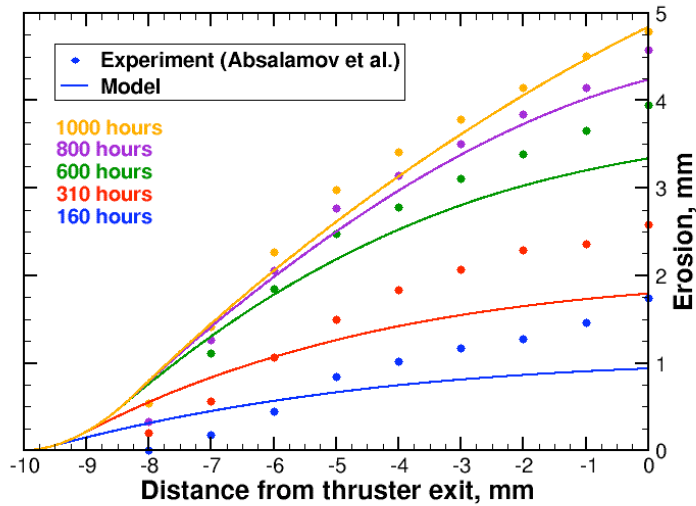
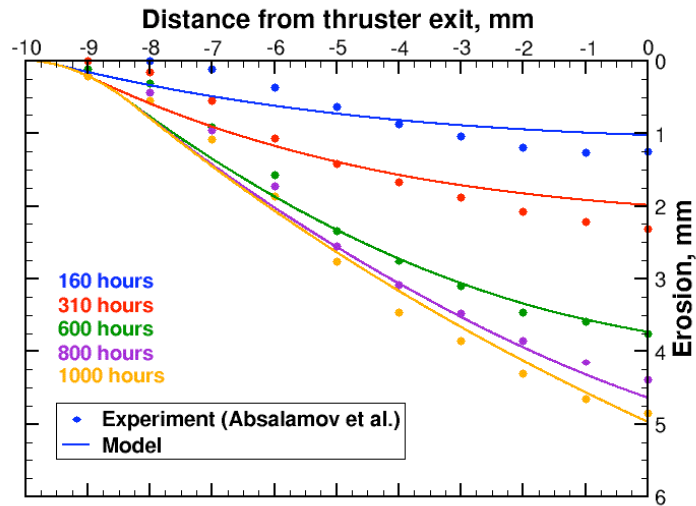


Figure 17. Wall erosion profiles for the SPT-100 Hall thruster: inner wall (upper); outer wall (lower) (from Yim et al. [74]).

